Validation of Simulation Results on a Scaled Roller Rig

Moritz Gretzschel and Alfred Jaschinski

April 16, 2002

0.1 INTRODUCTION

0.1.1 Application of roller rigs

The application of roller rigs to research into vehicle dynamics and the development of high-speed trains and other railway vehicles have become more widespread in recent decades. Both full scale and model rigs were used in the development of the bogies for the Shin Kansen in Japan in the 1950s at the Railway Technical Research Institute, and their use has increased since.

Full scale roller rigs offer the advantages that the experiments are independent of weather conditions, individual phenomena can be investigated, the experiments and the constraints as well as the particular conditions are reproducible. Though there are considerable differences between the dynamics of railway vehicles on roller rigs and on real tracks, these rigs have proved useful for both basic research and for development of innovative designs and particular investigations for the optimisation of suspensions and vehicle components. The emphasis is usually laid on tangent track experiments in order to obtain results for running stability and ride comfort on irregular tracks.

Model roller rigs and test tracks have been used to validate theory and to investigate new designs of vehicle. The obvious advantage of models over full scale is their low cost, ease of making modifications and ease of handling. If used for the investigation of new designs then the model requires dynamic scaling so that dynamic similitude is achieved and enabling measurements taken on the model to be applied to full scale practice.

Though the use of roller rigs has proved to be useful, they represent an incomplete simulation of the motion of a vehicle on the track. The differences involved in the application of roller rigs are discussed in [1].

The principle of a typical full scale roller rig

The wheel of a railway vehicle exerts forces on the rail as it rotates:

- vertical forces which result from the total load and the vertical dynamics of the railway vehicle;

- horizontal forces which stem from drive and braking in the direction of running, and laterally to the direction of running from the guidance behaviour.

The roller rig simulates the endless track by means of a steel roller. Two rollers which are arranged in accordance with the gauge - building a so called basic cell - can take one wheelset. The roller apexes of the basic cells are usually profiled according to UIC-60 rail profile.

To simulate track conditions, the rotating rollers can be

1

- separately moved in the y- and z- direction within about $\pm 10mm$ and turned about the x- and z-axis within ± 1 by actuators to simulate track geometry found in reality; where x is the axis pointing into the driving direction, z is the vertical and y the lateral axis of the orthogonal coordinate system,

- driven and braked to influence the forces transferred between wheel and roller.

Furthermore the rollers can be tilted about a common longitudinal (x-) axis so that a run with cant deficiency is simulated.

The distances between the individual basic cells can be adapted to the wheelsets of typical railway carriages.

0.1.2 Motivation and purpose of scaled roller rigs

Scaled roller rigs were developed to reproduce the fundamental dynamic behaviour of the full size railway vehicle in laboratory conditions so that measurements could easily be made under controlled conditions and the effects of certain changes to the vehicle demonstrated and understood, with the advantages that

- manufacturing of the scale rig and test vehicle causes rather low expense,

- handling and maintenance are comparatively easy,

- a lot of vehicle parameters can be changed with tolerable effort.

However, there are also inconveniences and disadvantages since similarity with respect to the complete range of the physical behaviour, as for instance to satisfy the conditions for both dynamic and elastic similarity, causes design problems. This matter will be treated later on in the section about scaling.

The fundamental ideas of similarity trace back to the work of O.Reynolds [2], [3], or even earlier. Analogous to Reynold's approach, similarity of mechanical systems with respect to dynamic behaviour and elastic deformation can be defined.

Small scale testing of railway vehicles on scaled roller rigs has been carried out for different purposes, for purposes including the verification and validation of simulation models, the investigation of fundamental railway vehicle running behaviour (non-linear response, as limit cycles, etc.), for the development and testing of prototype bogie designs with novel suspensions in order to support field tests and computer simulations and last but not least for teaching and demonstration of railway vehicle behaviour. Small scale tests at several institutions have proven that under laboratory conditions, influences of parameters can be revealed which often can not be separated from stochastically affected measurements of field tests which is of course also true for full scale rigs.

Particularly, when the non-linear running behaviour of railway passenger cars is studied, experiments become exceptionally important for the validation of modelling and prediction of the dynamical response. Especially in wheel-rail dynamics the non linear contact force laws play a dominant role for vehicle hunting which is caused through a bifurcation of the systems equation's solution into a periodic solution (limit cycle). Therefore, a scaled roller rig and a scaled bogie model have been built at DLR in order to perform measurements for validation of modelling and verification of parts of the developed software, see figure 1. The emphasis of these first investigations was to obtain fundamental knowledge about modelling and experimental methods in wheel-rail dynamics.
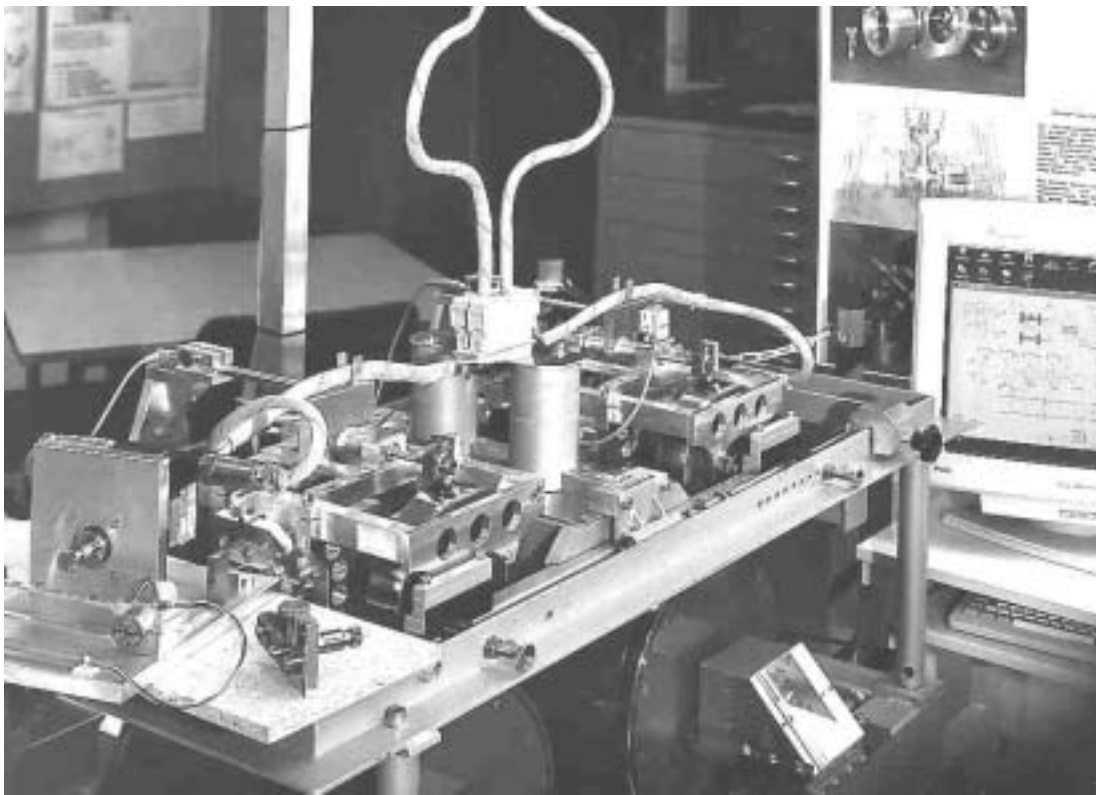

Figure 1: DLR scaled roller rig with experimental vehicle

After the Investigations on limit cycle behaviour with the above mentioned bogie model had been finished, [4], DLR started with the design of unconventional wheelset concepts and fundamental research in this area, [5].

3

0.2 THE SCALING PROBLEM OF ROLLER RIGS

0.2.1 General definitions

Similarity laws and the correlated problem of scaling are of particular interest for the transformation of experimental results from a scaled model to the full scale design. As previously mentioned, an early application of similarity laws was made by Reynolds, [2], [3], to the problem of viscous flow. Today, similarity laws are applied to a wide variety of engineering problems, from hydrodynamics, [6], flight dynamics, chemical process dynamics, [7], to design tasks in mechanical engineering.

There are various possible approaches to scaling. Early workers used the methods of dimensional analysis to establish several dimensionless groups from which the scaling factors could be derived [8] [9] [10], others first derive the equations of motion and then calculate scaling factors required for each term to maintain similarity. This later method is known as inspectional analysis and depends on good understanding of the equations of motion.

Choice of material properties is also a big factor in the scaling method used and also influences the loading conditions required for similarity. British Rail used aluminium wheels and rollers; [8], Matsudaira in Japan used steel, [10], and Sweet et al used plastic, [11]. In the example detailed here steel wheels and rails are used.

The starting point for the following considerations to define dynamic similarity of railway vehicles, is the geometric scaling, i. e. the definition of the length scaling factor

$$\varphi_l = \frac{l_1}{l_0} \tag{1}$$

where l_1 is a characteristical length of the full scale and l_0 a characteristical length of the scale model. In the same way a time scaling factor

$$\varphi_t = \frac{t_1}{t_0} \tag{2}$$

can be defined. With these definitions, scaling factors for cross section, φ_A, volumina, φ_V, velocity, φ_v, and acceleration, φ_a, follow:

$$\varphi_A = \varphi_l^2 \tag{3}$$
$$\varphi_V = \varphi_l^3 \tag{4}$$
$$\varphi_v = \frac{\varphi_l}{\varphi_t} \tag{5}$$
$$\varphi_a = \frac{\varphi_l}{\varphi_t^2} \tag{6}$$

When the density scaling φ_ρ is

$$\varphi_\rho \;=\; \frac{\rho_l}{\rho_0} \tag{7}$$

then scaling factors for mass, φ_m, moment of inertia, φ_I, and inertial force, φ_F, can be derived,

$$\varphi_m \;=\; \varphi_\rho \cdot \varphi_l^3 \tag{8}$$

$$\varphi_I \;=\; \varphi_m \cdot \varphi_l^2 \tag{9}$$

$$\varphi_F \;=\; \frac{m_1 a_1}{m_0 a_0} = \varphi_m \cdot \varphi_a = \frac{\varphi_\rho \varphi_l^4}{\varphi_t^2} \tag{10}$$

For further discussions we need:

- φ_T, scaling factor of creep forces, according to Kalker's theory of rolling contact, [12],

- φ_{ab}, scaling factor related with the size $e = \sqrt{ab}$ of the contact ellipse between wheel and rail,

- φ_E, scaling factor for Young's modulus,

- φ_ν, scaling factor for Poisson's ratio,

- φ_ε, scaling factor for strain

- ϕ_σ, scaling factor for stress

- φ_μ, scaling factor of friction coefficient μ,

- φ_c, scaling factor for stiffness,

- φ_d scaling factor for damping

- φ_f, scaling factor for frequency

0.2.2   The scaling strategy

Since DLR was involved in the development of simulation software for railway vehicle dynamics, including particularly also non-linear lateral dynamics (hunting) caused by bifurcation of the describing differential equations into a periodic solution (limit cycle), the scaling of the roller rig has been performed first of all with respect to similarity of this non-linear phenomenon.

Therefore, the starting point for this special scaling (for other scaling strategies see [1]) is the differential equation which describes the non-linear lateral dynamical behaviour of a single wheelset, suspended to an inertially moving body.

Such kind of differential equation has been derived in [4] for a wheelset with conical wheel profiles which does not influence the scaling procedure. The first component of this system of two coupled equations is as follows:

$$\frac{m}{\chi}\ddot{y}_w = \frac{I_y\Gamma v}{\chi r_0}\dot{\psi}_w - \frac{mgb_0}{\chi}y_w - \frac{c_y}{\chi}y_w + T_y + T_x\psi_w \tag{11}$$

Using the same symbols as already declared in the previous section, the non declared symbols denote:

I_y the wheelset's rotational moment of inertia
T_x the longitudinal creep force
T_y the lateral creep force

$\Gamma \quad = \frac{\delta_0}{l_0 - r_0\delta_0}$

δ_0 the cone angle

$\chi \quad = \frac{\Gamma l_0}{\delta_0}$

$b_0 \quad = 2\Gamma + \Gamma^2(R_R + r_0)$

R_R the profile radius of the rail head

Multiplying the scaleable parameters and variables in equation (11) with the previously defined scaling factors and arranging, results in:

$$\frac{m}{\chi}\ddot{y}_w = \frac{I_y\Gamma v}{\chi r_0}\dot{\psi}_w - \frac{mgb_0}{\chi}y_w\frac{\varphi_t^2}{\varphi_l} - \frac{c_y}{\chi}y_w\frac{\varphi_c\varphi_t^2}{\varphi_m} + (T_y + T_x\psi_w)\frac{\varphi_T\varphi_t^2}{\varphi_m\varphi_l} \tag{12}$$

The scale wheelset behaves dynamically similar to the full scale one, if the equations (11) and (12) coincide. This requires that the following conditions hold:

$$\frac{\varphi_t^2}{\varphi_l} = 1 \quad \Rightarrow \quad \varphi_v = \sqrt{\varphi_l}, \text{velocity scaling}$$

$$\frac{\varphi_c\varphi_t^2}{\varphi_m} = 1 \quad \Rightarrow \quad \varphi_c = \varphi_\rho\varphi_l^2, \text{stiffness scaling} \tag{13}$$

$$\frac{\varphi_T\varphi_t^2}{\varphi_m\varphi_l} = 1 \quad \Rightarrow \quad \varphi_T = \varphi_\rho\varphi_l^3, \text{creep force scaling}$$

Especially the first condition in (13) demonstrates that the velocity scaling cannot freely be choosen if similarity to lateral dynamics is demanded. This result is identical to that of Matsudaira et al, [10], from investigations carried out in 1968 at the RTRI of the Japanese National Railways.

From the constraint equations (a relation between the normal forces, the gyroscopic, gravitational, applied and creep forces, see [4]), with the above used

method, the scaling factors for the constraint (normal) forces, N, the mass and the creep forces result as follows:

$$\varphi_N = \varphi_m = \varphi_T = \varphi_\rho \varphi_l^3 \tag{14}$$

This result implies for the scale of the friction coefficient μ:

$$\varphi_\mu = 1.$$

Assuming, that Kalker's non-linear theory of rolling contact ends up with Coulomb's law of dry friction, we have to notice that for the rolling contact when the creepage saturation is not complete, dynamic similarity together with geometric similarity of the contact ellipse is required for the similarity of Kalker's creep forces. This yields a very incisive condition for the density scale φ_p, the remaining parameter which can be changed, since

$$\varphi_E = \varphi_\nu = 1$$

is required. From Kalker's Theory the relation between force and contact ellipse scaling is

$$\varphi_T = \varphi_{ab} \quad . \tag{15}$$

With

$\varphi_{ab} = (\varphi_N \varphi_l)^{2/3}$, and $\sqrt{\varphi_{ab}} = \varphi_e$, the scale of the contact ellipse mean radius, equation (15) becomes

$$\varphi_e^3 = \varphi_N \varphi_l = \varphi_\rho \varphi_l^4 \quad . \tag{16}$$

Assuming geometric similarity for the contact ellipse, $\varphi_e = \varphi_l$, equation (16) yields the condition for the density scale

$$\varphi_\rho = \frac{1}{\varphi_l} \quad . \tag{17}$$

To realize this density scaling together with a geometrical scaling factor of $\varphi_l = 5$ is nearly impossible. On the other hand, exact geometrical similarity of the contact ellipse (which is important for the creep forces when they are not saturated) seems to be not necessary when the wheelset is in the state of a limit cycle. During this non-linear state, creep forces are most of the period of a cyle saturated to $\mu \cdot N$ where the size of the contact ellipse has no influence on the creep forces.

Therefore, the following compromise for the density scaling seems to result in a rather good approximation for the dynamical similarity with respect to limit cycles: Instead of the required density scale of

$$\varphi_\rho = \frac{1}{5}$$

(for exact contact ellipse and creep force scaling), the scaling factor for the density was set to

$$\varphi_\rho = \frac{1}{2}$$

which can be reached easily and has proven for good experimental results. Then for the scale of the contact ellipse the following relation is valid:

$$
\begin{array}{ccccc}
\varphi_e = 5 & \leq & \varphi_e = 6.786 & \leq & \varphi_e = 8.55 \\
\Downarrow & & \Downarrow & & \Downarrow \\
\varphi_\rho = 1/5 & & \varphi_\rho = 1/2 & & \varphi_\rho = 1 \\
\text{perfect density} & & \text{compromise} & & \text{unscaled density}
\end{array}
$$

With

$$\varphi_l = 5$$

and the above mentioned compromise for the density scale, the other scaling factors can be determined as follows:

$$
\begin{array}{lcccl}
\varphi_v & = & \sqrt{\varphi_l} & = & \sqrt{5} \qquad \text{Velocity} \\[2mm]
\varphi_t & = & \frac{\varphi_l}{\varphi_v} & = & \sqrt{5} \qquad \text{Time} \\[2mm]
\varphi_a & = & \frac{\varphi_l}{\varphi_t^2} & = & 1 \qquad \text{Acceleration} \\[2mm]
\varphi_m = \varphi_T = \varphi_N = \varphi_F & = & \varphi_\rho \varphi_l^3 & = & 62.5 \qquad \text{Mass and forces} \\[2mm]
\varphi_1 & = & \varphi_\rho \varphi_l^5 & = & 1562.5 \qquad \text{Moment of inertia} \\[2mm]
\varphi_c & = & \varphi_\rho \varphi_l^2 & = & 12.5 \qquad \text{Spring stiffness} \\[2mm]
\varphi_d = \frac{\varphi_\rho \varphi_l^3}{\varphi_v} & = & \varphi_\rho \varphi_l^{5/2} & = & 27.9508 \qquad \text{Viscous damping} \\[2mm]
\varphi_f & = & \frac{\varphi_v}{\varphi_l} & = & \frac{1}{\sqrt{5}} \qquad \text{Frequency} \\[2mm]
\varphi_\mu & = & \frac{\varphi_T}{\varphi_N} & = & 1 \qquad \text{Coefficient of friction} \\[2mm]
\varphi_e & = & (\varphi_N \varphi_l)^{1/3} & = & 6.786 \qquad \text{Contact ellipse}
\end{array}
$$

Typical parameters

Table 1 shows the relevant parameters for the generic two-axle 1/5-scale test vehicle and the corresponding values for the full scale vehicle using the scaling strategy described above.

Table 1: Typical parameters for the generic test vehicle.

Parameter	Full-size	1/5 scale
Wheelset structure		
structure frame mass	487.5 kg	7.8 kg
wheel mass	281.25 kg	4.5 kg
Axle mass	275 kg	4.4 kg
structure frame roll inertia	218.75 kgm^2	0.14 kgm^2
structure frame pitch inertia	103.125 kgm^2	0.066 kgm^2
structure frame yaw inertia	192.19 kgm^2	0.123 kgm^2
wheel rotational inertia	51.56 kgm^2	0.033 kgm^2
Axle rotational inertia	3.125 kgm^2	0.002 kgm^2
Vehicle frame		
frame mass	2037.5 kg	32.6 kg
frame roll inertia	1403.13 kgm^2	0.898 kgm^2
frame pitch inertia	1339.06 kgm^2	0.857 kgm^2
frame yaw inertia	2342.19 kgm^2	1.499 kgm^2
Wheels		
wheel diameter	1.0 m	0.2 m
gauge	1.435 m	0.287 m
wheelbase	2.5 m	0.5 m
Primary suspension		
longitudinal stiffness	8.3 10^5 Nm^{-1}	6.64 10^4 Nm^{-1}
lateral stiffness	8.3 10^5 Nm^{-1}	6.64 10^4 Nm^{-1}
vertical stiffness	5.9 10^7 Nm^{-1}	4.73 10^6 Nm^{-1}
Normal force	11496 N	183.94 N
Speed	v	$v/\sqrt{5}$

0.3 SCALED SIMULATION AND CONTROLLER DESIGN

0.3.1 Motivation

The motivation for the use of scaled model experiments can be manifold, as already stated in section 0.1.2. Most common purposes can be

- Experimental verification of simulations, methods or theories with reduced experimental effort

- Estimation of Parameters for full size vehicles by means of similarity laws

- Practical functional demonstration of vehicle developments

- Controller design for full size vehicles.

Whilst the first three points are self-evident, an example is given for the latter.

The integration of electronics and control into traditionally mechanical systems represents a radical change which has already affected railway industry. Future vehicles will be mechanically more straightforward, and the mechanical simplification may be made possible by using the synergies between different control tasks. A number of innovative concepts has been modelled and described in literature, but most of them are devoted to one singular control instead of taking into account other systems in the vehicle. Partially it is caused by insufficient capability of simulation tools used for the investigations. By means of complementary hardware experiments, simulation models can be validated, unknown parameters can be identified [13], and control laws and their feasibility and implementation can be tested.

But in order to simulate such systems correctly, it is necessary to model the complete mechatronic system not only because the passive system would no longer work sufficiently without controls, but also because one control system influences the other one in its sensing and its action. But computer simulation is not always sufficient for the design and verification of the control structures for such mechatronic vehicles. Concurrent and complementary hardware experiments can prove the feasibility and functionability of the controlled system under the influence of environmental influences and excitations. The implementation of the control laws by means of sensors, processors and actuators can be tested, and possible unexpected interactions can be detected.

As an example, a mechatronic wheelset concept has been developed by DLR [14] which directly interacts with the wheelset's friction forces and thus drastically changes the known running dynamics. This is achieved by the controlled transmission of a differential torque from one wheel to the other.

The main aim of this mechatronic wheelset is to solve the design conflicts between stability, curving performance, comfort and wear. As the controlled

wheelset runs stably by directly controlling the longitudinal slip forces there is more freedom to design its suspension to provide more comfort and not to restrict the ability to run through tight curves. Both wheel forces and friction power can be considerably reduced leading to less wear and less noise. By simplifying the suspension mechanically and combining traction and steering functionality a generation of unconventional, powerful and light railway vehicles becomes possible.

This leads to an integrated approach for tilting, traction and steering control. This is also sensible because several signals like ground speed, curve radius and lateral displacement are needed in all those control loops which influence each other in their determination.

0.3.2 Simulation and experiment

Model vehicles with the previously introduced mechatronic wheelset are being tested on the scaled roller rig of DLR, already briefly mentioned in section 0.1.2. The rig consists of two rollers with scaled UIC60 rails. Both rollers are coupled and synchronised by a timing belt and driven by a disc-rotor asynchronous motor. The experimental vehicles are suspended in longitudinal direction by a spring-damper-combination and can perform lateral oscillations with an amplitude of up to some 20mm, unless restricted by the wheel flanges.

Currently there are two generic experimental vehicles available. They are called generic because they can be freely adapted to a number of wheelset configurations, from the classic solid wheelset to independently rotating wheels and connection of the wheels by an arbitrary passive, semi-active or active torque coupling. On the first test vehicle this coupling is provided mechanically by a special gearbox, on the second vehicle electrodynamically by an individually controlled and independent drive motor for each wheel.

0.3.3 Steering principle

As a first approach a gearbox was developed that couples the two wheels of an axle in such way that the differential torque can be introduced from an external servo motor directly between the two wheels [15]. This superimpositional gearbox transmits the differential relative speed, and neglects the absolute speed. Therefore, the electric servomotor only interacts with the differential torque, and is not affected by eventual propulsion or braking torques. Thus, a relative motion of the two wheels of an axle purely occurs as the result of an asymmetric balance of the commanded differential torque and the frictional torques of both wheels.

The superimpositional gearbox represents only one possible solution for this principle. The mechanical coupling can be replaced by an electrodynamic one. In particular it is possible to use the same control schemes for axles with wheels driven independently by separate traction motors. The commanded differential

torque is superimposed to the propulsion or braking torque, allowing the investigation of active stabilisation combined with driving or braking. Nevertheless, special control strategies are needed to keep full control of the vehicle near the limit of adhesion. These experiments are executed using the second experimental vehicle equipped with one motor at each wheel. The motors with printed disk rotors are small enough to be fitted directly to the wheelset structure, and powerful enough to investigate traction up to the limit of adhesion. So this second vehicle represents a typical meachatronic approach of a mechanically simpler system offering more performance than the conventional electromechanical one.

0.3.4 Control and implementation

Design process

The controller is implemented on a digital signal processor (DSP) card housed in a PC. The state measurements are collected via a second DSP card and written to a database. The control laws are designed using a non-linear MBS simulation model. Figure 2 shows the SIMPACK simulation model of the test vehicle on the roller rig, corresponding to the experimental setup in figure 1.

The vehicle model consists of 15 rigid bodies with up to 6 degrees of freedom each and 30 dynamic joint states. It includes full three-dimensional nonlinear wheel-rail contact with friction forces calculated according to Kalker [12].
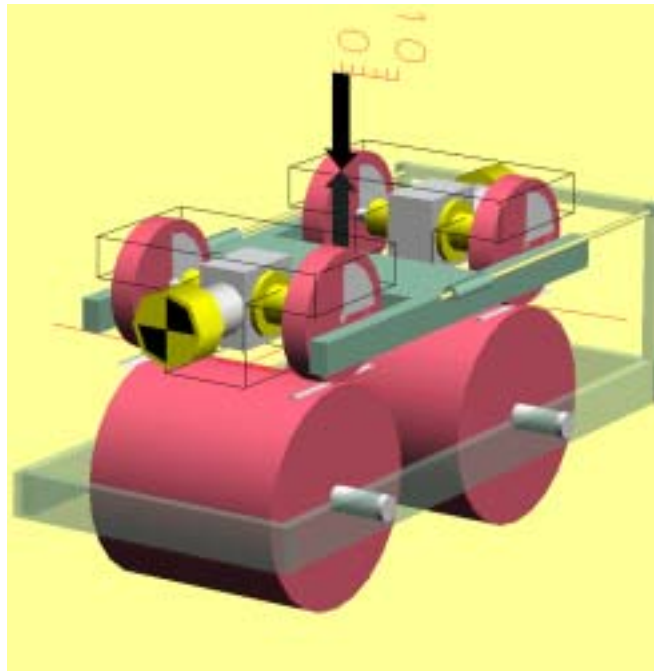

Figure 2: Multibody simulation model of roller rig and vehicle

The complete control circuit is designed using the block-oriented graphic user interface Simulink. Via the MATLAB Real Time Workshop this control law is translated automatically to C-code and downloaded to the digital signal processor controlling the vehicle. The control architecture and parameters can therefore be changed very fast, and the results are immediately visible from the behaviour of the test vehicle, see figure 3.

Using the SIMPACK-MATLAB/Simulink interface, the non-linear and three-dimensional model of the complete mechatronic system can be simulated and the control loop can be optimised. After the automatic transfer of the controller code to the DSP the test vehicle is ready to validate the controller and to prove the feasibility and stability of the system in a real hardware environment.
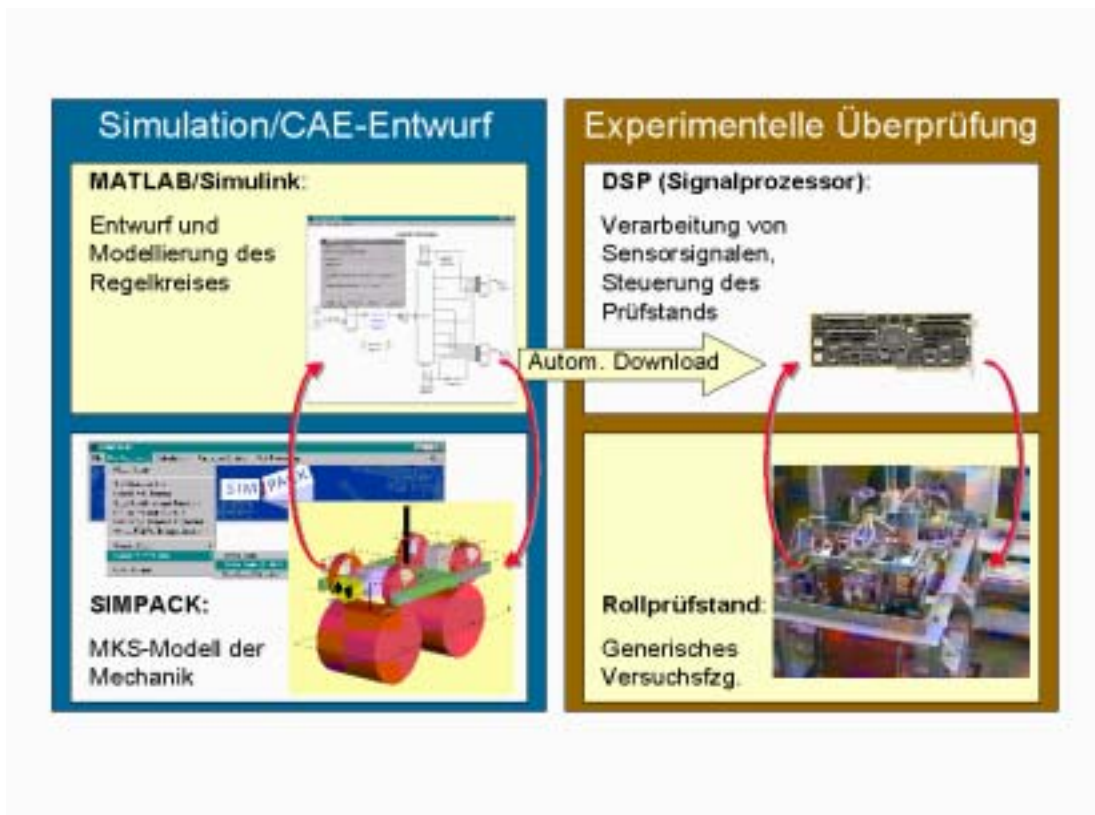

Figure 3: Design Process by simulation and complementary hardware experiments

Lateral control

A simple PID-controller was sufficient for first tests on the roller rig. This controller is fed with the lateral displacement and the vehicle yaw angle estimated from the relative rotation of the wheels. The yaw velocity measured directly is used for stabilisation.

Figure 4 shows a simplified block diagram of a control circuit for wheel motor axles. The lateral displacements of leading and trailing axle are either directly measured (for first tests) or calculated from relative rotational speed and travelling speed. From these two values the lateral displacement and yaw angle of the vehicle main frame are calculated, scaled individually and then added. The scaled yaw rate of the leading axle unit is also added for stabilisation purpose. This sum is then fed to a PID controller which delivers the amount and direction of the desired differential torque. For comparison it can be switched between external or onboard sensors and between controlled or manually set differential torque at any time. So a solid wheelset can be simulated by setting the coupling torque to its maximum value, a pair of independently rotating wheels by setting it to zero.
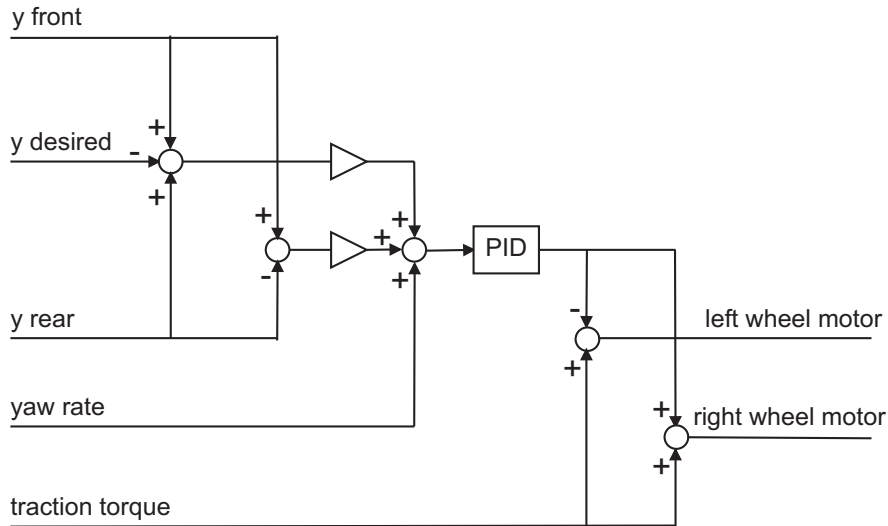

Figure 4: Simplified block diagram of control circuit

The scaling factors of the various input values and the P, I and D components of the controller were determined by MBS-simulations of vehicle and roller rig modelled with SIMPACK. Due to earlier parameter identification studies [13] the SIMPACK model is very well verified. For this reason the experiment worked satisfactorily right from the beginning using these parameters.

There are special control strategies needed to allow the steering of the axle up to the limit of adhesion and to be able to cope with adverse situations (like extreme gradients or curves) in which a choice between full steering or full traction capability is inevitable.

Theoretically, the lowest friction power, which is the main cause of wheel- and rail wear, can be achieved if the axle is running strictly in radial position. In this case the lateral creep and thus friction power would become zero. But in this case all lateral forces have to result from the lateral components of the normal forces (gravitational stiffness), and a small amount caused by the spin creepage,

resulting in a wheel-rail contact point of the outer wheel being very close to (or even on) the flange of the wheel. In spite of the low friction work, this strategy of a strictly radial position has several disadvantages. Near to the radial position the wheelset is very sensitive to small variations of the yaw angle. Fractions of one millirad cause large effects in lateral position. This means that the yaw angle would have to be measured and controlled extremely precisely which would be very difficult in reality. Another disadvantage is the outer flange running very close to the rail. Even small rail irregularities would cause a sudden hard contact between flange and rail, drastically deteriorating the comfort.

Therefore a different control strategy was chosen. The main aim is not to keep the axle exactly radial, but to keep it well away from flange contact. The relative torque is controlled such that the yaw angle causes lateral friction forces just compensating the cant deficiency forces. This improves the passenger comfort in lateral direction. The slight increase of friction work compared to the radial position is still very low (the wear index being in a non-critical region) compared to conventional passive running gears.

0.3.5   Transfer of results to full scale models

As pointed out in [1], results achieved using roller rigs can never be fully identical to those gained by field test on real track. The contact geometry between wheel and roller is geometrically different from that between wheel and rail, generally adding instability to the roller rig experiment and resulting in a lower critical speed. Not all types of track excitations can be fully reproduced on roller rigs, depending on the design of the setup. The same applies to curving which is generally difficult to be simulated on a roller rig because of the centrifugal forces and since the different distance to be travelled on inner and outer rail is neglected by most roller rigs.

The general effects and critical states however, no matter whether occurring on full size or scaled roller rigs, can be well compared to real scenarios. Here another advantage of combined experiments and multibody simulations becomes evident: If the simulation model is validated for certain typical manoeuvres on the roller rig, an extrapolation to simulation scenarios going beyond the possibilities of the rig is possible. For this case, it is desirable if the simulation program is capable of correct modelling the rail contact either on the track or on the rollers.

In addition, the control laws developed on scaled models can be directly adopted to the full size case, as long as the actuator parameters are consistently scaled: For the example of the mechatronic wheelset described in this section, the controller was designed for the scaled model vehicle by means of a simulation model of the scaled vehicle, and directly transferred to the experimental setup. In a second step, a full size simulation model of a rail vehicle was designed. In order to present the advantages of the mechatronic concepts, an advanced vehicle concept had been selected. It is an articulated vehicle consisting of three units

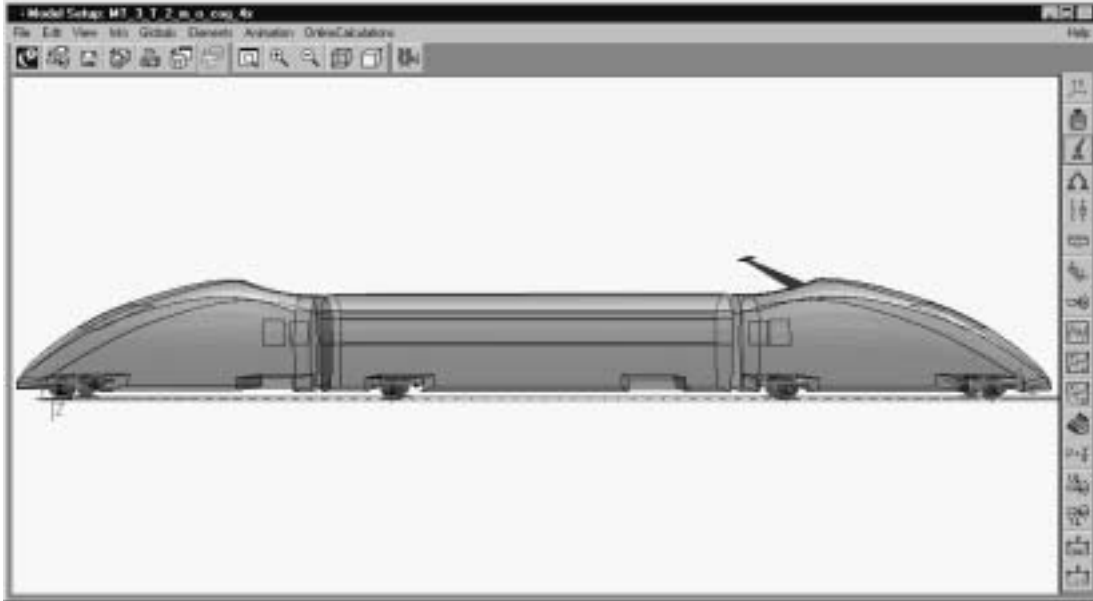supported by four axles, see Figure 5.

Figure 5: Virtual demonstrator vehicle

The vehicle is equipped with a single axle bogie construction. Each bogie carries a differential torque controlled active wheelset. The controllers of the wheelsets are equipped with the same control laws designed using the scaled model before. Due to the consistent scaling, the full size vehicle simulation model achieves the same behaviour and performance as expected, without any problems of adapting the controller to the bigger scale. Important outputs, such as the power consumption by the actuators, were directly comparable between the scaled simulation model, the scaled experimental vehicle and the full size simulation model when scaled accordingly to the similarity laws.

0.4 OUTLOOK

Roller rigs, full size and scale, are being used by researchers and railway organisations around the world to assist in the understanding of the behaviour of railway vehicles and the development of faster, safer and more efficient railways. Roller rigs have contributed to many current designs of railway vehicles. For model rigs as a major rule, it can be stated that perfect scaling with respect to dynamic together with elastic response is nearly impossible when the density of the material is the only material parameter that can be altered, since then the relation between the density scaling and the geometrical scaling holds,

$$\varphi_p = \frac{1}{\varphi_l}.$$

In this case, a compromise as described in the scaling strategy has to be considered. In general, scaling with tolerable effort of design and manufacture is strongly related to the emphasis of the vehicle's dynamics to be represented on the roller rig.

The potential offered by advanced computing tools and intelligent control methods means that scaled and full scale roller rigs can continue to offer advantages over field testing. They also provide data in new areas when computer methods are not yet proven or when working outside the envelope of validation. Although field testing of prototype vehicles will never be completely eliminated, roller rigs will continue to be a valuable tool to researchers and developers as an intermediate stage between computer simulations and track testing.

Bibliography

[1] Alfred Jaschinski, H. Chollet, S. Iwnicki, A. Wickens, and J. von Würzen. The application of roller rigs to railway vehicle dynamics. *Vehicle System Dynamics*, 31:345–392, 1999.

[2] O. Reynolds. An Experimental Investigation of the Circumstances which Determine wether the Motion of Water shall be Direct or Sinous, and the Law of Resistance in Prallel Channels. *Phil. Trans. R. Soc.*, 174:935–953, 1883.

[3] O. Reynolds. On the Dynamical Theory of Incompressible Vicous Fluids and the Determination of the Criterion. *Phil. Trans. R. Soc.*, 186:123–164, 1895.

[4] Alfred Jaschinski. *On the application of similarity laws to a scaled railway bogie model*. PhD thesis, TU-Delft, 1990. and DLR-FB Oberpfaffenhofen 90-06.

[5] Alfred Jaschinski and H. Netter. Non-linear dynamical investigations by using simplified wheelset models. In G. Sauvage, editor, *The Dynamics of Vehicles on Roads and Tracks. Proc. 12th IAVSD Symposium, Lyon, France, August 26-30, 1991*. Swets & Zeitlinger, Amsterdam/Lisse, 1992.

[6] L. Milne-Thomson. *Theoretical Hydrodynamics*. 3rd edition, London, 1955.

[7] W. Matz. *Anwendung des Ähnlichkeitsgrundsatzes in der Verfahrenstechnik*. Springer, Berlin, Göttingen, Heidelberg, 1954.

[8] A. H. Wickens. The dynamics of railway vehicles on straight track: fundamental considerations of lateral stability. In *Proc. I. Mech. E.*, volume 180, pages 29–44, 1965.

[9] R. Illingworth. Railway wheelset lateral excitation by track irregularities. In *Proc. 5th VSD-2nd IUTAM Symposium, Vienna, Austria, September 19-23, 1977*. Swets & Zeitlinger, Amsterdam, 1978.

[10] T. Matsudaira, N. Matsui, S. Arai, and K. Yokose. Problems on hunting of railway vehicle on test stand. *Trans. A.S.M.E. J. of Eng. in Industry*, 91(3):879–885, 1969.

[11] L. M. Sweet, J.A. Sivak, and W. F. Putman. Non-linear wheelset forces in flange contact, part 1: Steady State Analysis and Numerical Results, part 2: Measurement using Dynamically scaled Models. *Journal of Dynamic Systems, Measurement and Control*, 102:238–255, 1979.

[12] J.J. Kalker. *Three-Dimensional Bodies in Rolling contact*. Kluwer Academic Publishers, Dordrecht, Boston, London, 1990.

[13] F. Grupp. *Parameteridentifizierung nichtlinearer mechanischer Deskriptorsysteme mit Anwendungen in der Rad-Schiene-Dynamik*. Dissertation, VDI Fortschritt-Berichte, Reihe 8: Meš-, Steuerungs- und Regelungstechnik, Nr. 550, VDI Verlag, Düsseldorf, 1995.

[14] Moritz Gretzschel and Alfred Jaschinski. *Ein mechatronisches Radsatzkonzept zur aktiven Beeinflussung der Fahrdynamik von Schienenfahrzeugen*, volume ISBN 3-18-091392-4 of *VDI Berichte 1392*. VDI-Tagung: Der spurgeführte Verkehr der Zukunft, Hamburg, 18./19.06.1998, 1998.

[15] Moritz Gretzschel. Konzeption und Konstruktion einer aktiven Torsionsverbindung für einen generischen Eisenbahnradsatz. Master's thesis, Lehrstuhl für Konstruktion im Maschinenbau, TU-München and DLR, Diploma Thesis No. 674, 1995.